Density of Newly Synthesized Plasma Membrane Proteins in Intracellular Membranes. I. Stereological Studies

G. GRIFFITHS, G. WARREN, P. QUINN, O. MATHIEU-COSTELLO,* and H. HOPPELER‡

*European Molecular Biology Laboratory, 6900 Heidelberg, Federal Republic of Germany; *Anatomy Institute, University of Bern, Bern Switzerland; ‡Department of Medicine M-023, University of California, San Diego*

ABSTRACT As the spike proteins of Semliki Forest virus (SFV) pass from their site of synthesis in the endoplasmic reticulum (ER) to the cell surface, they must be concentrated and freed from endogenous proteins. To determine the magnitude of this sorting process we have measured the density of spike proteins in membranes of the intracellular transport pathway. In this first paper, using stereological procedures, we have estimated the surface areas of the ER, Golgi complex, and plasma membrane of infected and mock-infected baby hamster kidney cells. First, we estimated the mean cell volume in absolute units. This was done using a novel in situ method which is described in detail. Infection by SFV was found to have no effect on any of the parameters measured. In the accompanying paper (Quinn, P., G. Griffiths, and G. Warren, 1984, *J. Cell Biol.*, 2142–2147) these stereological estimates were combined with biochemical estimates of the amount of spike proteins in ER, Golgi complex, and plasma membrane to determine the density in the membranes of these compartments.

Most, if not all, of the spanning membrane proteins of the endoplasmic reticulum (ER)[1], Golgi complex, lysosomes, and plasma membrane originate from the same compartment, the rough ER (7, 17, 21). The mechanisms by which these membrane proteins, all inserted co-translationally into the rough ER membrane, become concentrated and sorted faithfully to their correct target organelles are far from understood. At present this sorting or selection process can only be described in qualitative terms. One can for example conclude that the concentration of plasma membrane protein precursors in ER and Golgi complex is far lower than it is in the plasma membrane itself, but the available data is just not sufficient to express these concentrations in quantitative terms (13, 15).

As a model for the biogenesis of plasma membrane proteins, we have used the spike glycoproteins of Semliki Forest virus (SFV). After viral infection, the cellular machinery for protein synthesis and intracellular transport is entirely devoted to the making and transporting of large quantities of a few specific viral proteins, making both biochemical and morphological studies relatively easy. In a previous study we have followed the pathway and kinetics of intracellular transport of the two membrane-spanning glycoproteins (E1 and p62) of this virus in baby hamster kidney (BHK) cells by a combination of biochemical and immunocytochemical techniques (8–10, 19). Our results showed that the viral membrane proteins move sequentially from the rough ER through the stacks of Golgi cisternae to the plasma membrane. Furthermore, the immunocytochemical data indicated that the viral membrane proteins were found uniformly throughout the rough ER and Golgi membranes but at the plasma membrane, they were mostly restricted and concentrated in those regions where virus budding had occurred.

The aim of this, and the accompanying paper (20) was to determine the density of the spike proteins in the ER and Golgi membranes using a combination of morphological and biochemical techniques. The stereological approach, the topic of this first paper, provided us with estimates of the absolute surface areas of these compartments per average BHK cell. The biochemical approach, which is dealt with in the second paper, allowed us to estimate the total number of SFV spike protein molecules in the total fraction of ER and Golgi membranes per average BHK cell. Since our reference unit was the same for both studies it is simple to estimate the densities (number of molecules per unit surface area of membrane) of these glycoproteins in the ER and Golgi membranes.

[1] *Abbreviations used in this paper:* BHK, baby hamster kidney; ER, endoplasmic reticulum; SFV, Semliki Forest virus.

THE JOURNAL OF CELL BIOLOGY · VOLUME 98 JUNE 1984 2133–2141

Stereological methods have been used to quantitate the same cell compartments in hepatocytes (26) and exocrine pancreas cells (1). In these studies the volume and surface densities of interest could be expressed in absolute units by reference to the total volume of the respective organs. For BHK cells, which grow in culture, we developed a novel approach that allowed us to estimate the mean cell volume in situ. This parameter was then used as our reference frame to determine the absolute quantities of the relevant compartments. Having obtained this, the volume densities of cytoplasm per cell followed by Golgi complex and ER volumes per volume of cytoplasm were determined. Finally the surface densities of ER, Golgi complex, and plasma membrane were estimated with respect to the volume of the respective compartment. These estimates were made on both infected and mock-infected cells.

METHODS AND RESULTS

Cells: BHK-21 cells were grown and infected with SFV as described previously (8) and used 6 h after infection. When pellets of cells were required, 50 μg/ml proteinase K in PBS at 0°C was used to remove the monolayer from the dish, a procedure taking ~5 min (8). The cells were then sedimented by centrifugation for 1 min at 4,000 *g*.

The procedure for preparing cells for embedding and subsequent morphometric analysis was to plate out identical numbers of cells into dishes and to monitor the growth until the cells were confluent. This was, a density between 2.3- and 2.6 × 10^5 cells/cm^2. Ten of these dishes were used to count the number of cells (see below) and the remaining two were used for stereological analysis after fixation with glutaraldehyde. Fixation was found to have no effect on cell density.

Light Microscope Preparation: Estimation of Number of Cells per Surface Area of Dish: To estimate the number of cells per surface area of petri dish, we used light microscopy. The best procedure we found for doing this was to use a fluorescent dye that binds DNA and clearly delineates the nuclei. Hoechst dye number 33258 (1 mg/ml in PBS) was added to the monolayer in 5-cm petri dishes, and incubated for 10 min at 37°C. The cells were then viewed and photographed directly on the plate using a Zeiss light microscope equipped with a blue filter and a × 6.3 objective lens. The images were enlarged photographically approximately 10 times.

Electron Microscopic Preparation: Cells, either as monolayer or pellet, were fixed for 30 min with 1% glutaraldehyde in 0.1 M PIPES buffer, pH 7.0 containing 5% (wt/vol) sucrose. This and all subsequent steps were carried out at room temperature. The preparations were washed three times (10 min total) with 0.1 M PIPES buffer, pH 7.0 containing 10% (wt/vol) sucrose. The tissues were then treated for 15 min with 2% O_5O_4 in 0.1 M sodium cacodylate, pH 7.0 containing 0.2% potassium ferricyanide and 5% (wt/vol) sucrose. After brief rinses in 0.1 M cacodylate buffer pH 7.0, 1% tannic acid in this buffer was added and left for 30 min followed by a 10-min rinse in 1% sodium sulfate in the same buffer (22). Ethanol dehydration commenced with 70% ethanol and took a total of 15–20 min. Monolayers were removed as a sheet using propylene oxide that, unlike ethanol, dissolves the plastic of the dish. In detail, at the 100% ethanol stage, increasing amounts of propylene oxide were added to the dish, with the simultaneous and gradual removal of the ethanol with a pipette. The monolayer was scratched into small squares (2–3 mm^2) using a scalpel, and aided by vigorous pipetting, the pieces of monolayer sheet came off the petri dish when the propylene oxide concentration became high enough. When thin sections of these embedded monolayers were examined in cross-section, it was apparent that a thin, electron-dense film of plastic always came off with the cells (Figs. 2 and 3). This enabled the top and bottom of the monolayer to be easily determined and also allowed us to relate the volume of the cell to the surface of the dish and hence to estimate the mean volume of the cell (see below). After the propylene oxide step the pieces of monolayer were pelleted at 13,000 *g* for 5 min and flat embedded in an Epon 812 mixture in such a way that the sheets were perpendicular to the cutting direction. This could easily be confirmed when the blocks were trimmed. Usually three to four such pieces of monolayer would be present in any one section (see Fig. 2). Care was taken to ensure that any piece that was not perpendicular (± 15°) was not sectioned. Silver-grey sections, estimated to be ~40 nm thick by the fold-procedure (23), were cut using a Reichert OMU3 ultramicrotome. These were mounted on 100 mesh copper grids having carbon-coated formvar films and were contrasted for 2–3 min with lead citrate solution. Cytochemical localization of glucose 6 phosphatase was carried out as described previously (10).

Stereological Analysis

Estimation of Mean Cell Volume: In a morphometric analysis each parameter is obtained as the ratio of two measurements, one estimating the size of the objects investigated, the other the size of the space in which they are contained (reference space). In most biological applications the organ volume is the primary reference space all subsequent parameter estimates are related to, whereas in cell cultures the mean cell volume seems to be the natural primary reference space. If the reference space does not remain constant under the experimental conditions, or if parameter estimates are to be obtained in absolute quantities, the volume of the reference space must be determined before tissue is processed for analysis. When dealing with organs, this is easily done by fluid displacement; for BHK-cell cultures growing in a monolayer, however, we had to devise an alternative approach to estimate the mean volume of a BHK-cell, $\bar{v}(c_0)$. BHK-cells grow as a monolayer on the surface of a plastic petri plate. As mentioned in Materials and Methods, our electron microscopic preparation technique is such that during the propylene oxide dehydration stage, a thin layer of the plastic is removed along with the cell monolayer (Fig. 2). This allows us to obtain $\bar{v}(c_0)$ by

$$\bar{v}(c_0) = \frac{V(c_0)}{N(c_0)} = \frac{V(c_0)}{S(d_0)} \div \frac{N(c_0)}{S(d_0)}, \quad (1)$$

where $V(c_0)/S(d_0)$ is cell volume, $V(c_0)$, per unit area of petri dish surface, $S(d_0)$, as obtained from electron micrographs of sectioned cell cultures (Fig. 3). This variable can also be viewed as representing the mean thickness of cells in the petri dish. $N(c_0)/S(d_0)$ is the number of cells, $N(c_0)$, per unit area of petri dish surface, $S(d_0)$, as obtained from the light microscopic analysis of the in situ cells. Note that the parenthesis c and d refers to the structural sets of cell and dish, respectively, whereas the subscript 0 denotes that these quantities were obtained on sampling level 0 (Fig. 1).

Estimation of Cell Number per Dish Surface: For the estimation of $N(c_0)/S(d_0)$ in a typical experiment, each of ten-6-cm petri dishes of cells, all identically plated, were subsampled by systematic quadrats, in a similar fashion as that shown by Cruz-Orive (6). Within each quadrat, the "forbidden line" unbiased counting rule was used (11). A total of 1,000–1,200 cell projections were counted for each plate. The standard error was typically found to be <10% of the estimated mean in each treatment. A calibration marker was photographed along with each roll of film and the magnification was measured accordingly. We could hence calculate the number of cells per square centimeter of dish surface.

Estimation of Cell Volume per Dish Surface: $V(c_0)/S(d_0)$ was estimated for control, mock-infected, and SFV-infected cells as ratio of sums over quadrats as follows:

$$\frac{V(c_0)}{S(d_0)} = \frac{A(c_0)}{B(d_0)}, \quad (2)$$

$$A(c_o) = \frac{a_o}{p_o} \cdot \sum_{i=1}^{m} P_i(c_o) \cdot M_i^{-2}, \quad (3)$$

and

$$B(d_o) = \frac{\pi}{2} \cdot \frac{a_o}{l_o} \sum_{i=1}^{m} I_i(d_o) \cdot M_i^{-1}, \quad (4)$$

where $A(c_0)/B(d_0)$ is the cell profile area, $A(c_0)$, per boundary length of petri dish trace, $B(d_0)$ (24). This is an unbiased estimate of $V(c_0)/S(d_0)$ because the section plane is not isotropically oriented with the surface (d_0) of the petri dish. In fact the sections were taken in such a way that the two planes would be approximately perpendicular to each other (within 15°) as described above. For a mathematical justification see reference 25 (equation 6.32).

In Eqs. 3 and 4, $P_i(c_o)$ is the number of test points inside BHK-cells in the i^{th} quadrat; $I_i(d_o)$ is the number of intersections of test line with the petri dish trace in the i^{th} quadrat; M_i is the magnification of the i^{th} quadrat; m is the total number of quadrats subsampled from five petri dishes; and p_o, l_o, a_o are the constants characterizing the fundamental figure of the test system (5).

Note that Eqs. 3 and 4 and the formulae in the Appendix deal with magnification corrections properly and allow one to handle the stereological data obtained via arbitrary, different coherent-test-systems (5). In Weibel's (25) nomenclature $p = 1$, $a = k_2d^2$, and $l = k_1d$ for the "coarse" points of a multipurpose test system.

Calculation of the Standard Errors of the Estimators: For all stereological variables the standard error of the estimates (SE) were calculated by pooling data from all quadrats of each treatment and by applying formulas for the standard error of ratios (4). The tissue within each micrograph (quadrat) was, therefore, taken as the primary sampling unit. This seems to be justified

when dealing with cultures of a single cell line. SE, hence denotes the variability among quadrats (cells). To test the significance of differences the Students t-test for independent samples was used; the level of statistical significance was set at the 5% level.

Sampling Model for BHK-cells: A multilevel sampling design was used to estimate the subcellular composition of BHK-cells (6). The cells were conceptually broken down as follows:

$$\underset{(c_0)}{\text{BHK-cell}} \supset \underset{(c_1)}{\text{cytoplasm}} \supset \underset{(c_2)}{\text{ER and Golgi volume}} \supset \underset{(\partial c_3)}{\text{ER and Golgi membranes,}} \quad (5)$$

where A ⊃ B means A contains B. The ratios of main interest were $V(c_2)$ and $S(\partial c_3)$, where V denotes volume, S surface area, and the boundary of the set c_3. These quantities thus read "volume of ER and Golgi" and "surface area of ER and Golgi membranes." A schematic representation of the sampling method used is shown in Fig. 1.

Sampling Protocol: To estimate the cell volume to petri-dish surface ratio, the sections were cut essentially perpendicular to the petri dish surface. It was assumed that the distribution of the relevant second and third level quantities was isotropic, uniform, and random with respect to the section plane. This assumption does not hold for the orientation of the plasma membrane however, which shows anisotropy with respect to the section plane. Hence, this parameter was estimated in cell pellets obtained after removing the cells from the petri-dish (Fig. 7).

One section was taken from each of five randomly chosen blocks from each treatment. In each of these sections (mounted on 100-mesh copper grids), 1 to 4 long ribbons of cells were present (Fig. 2). Each section was subsampled by systemic quadrats (SQ; 16) as follows: Beginning with an arbitrary window of the copper grid, each window was scanned to determine whether BHK-cells (the reference space, c_0) intersected the left grid bar. When the reference space complied with the a priori sampling rule the section was translated until the electron microscope screen was tangential to the grid bar and the cell in the center of the quadrat. A micrograph at a final magnification × 7,200 was then taken with a Philips electron microscope 400 on 35-mm film (level I; Fig. 2). The actual magnification was assessed with the aid of a calibration grid of parallel lines (1/2,160 mm apart). Without moving the section a second micrograph was then taken at a final magnification of × 22,000 (level II). Finally for level III (final magnification × 108,000), the section was systematically translated to the left and two micrographs were obtained from the nearest region containing ER including nuclear envelope, (Fig. 5) and a separate region containing Golgi (Fig. 6). Figs. 3, 4, and 5 are meant to provide a pictorial impression of the sampling procedure in that they show increasing magnification of the same cell.

Estimation of Parameters: To efficiently estimate the surface area of Golgi and ER membranes, BHK-cells were analyzed at three different levels of magnification as follows:

$$\bar{s}(\partial c_3) = \bar{v}(c_0) \cdot \frac{V(c_1)}{V(c_0)} \cdot \frac{V(c_2)}{V(c_1)} \cdot \frac{S(\partial c_3)}{V(c_2)}, \quad (6)$$

where $\bar{v}(c_0)$ was obtained as described in a previous section. The first level quantity $V(c_1)/V(c_0)$-volume of cytoplasm per BHK-cell volume was estimated at a total magnification of × 7,200; the complete formula is given in the appendix. The second level quantities $V(c_2)/V(c_1)$, volumes of ER and Golgi per volume of BHK-cell cytoplasm, were estimated at a final magnification of × 22,000. The third level quantities $S(\partial c_3)/V(c_2)$, surface area of ER and Golgi membranes per volume of ER and Golgi-apparatus, were estimated at a final magnification of × 108,000. The estimation of cell volume per unit area of petri dish surface was carried out as described in an earlier section. $S(c_0)/V(c_0)$, BHK-cell surface area per unit cell volume (level IIb) was estimated in BHK-cell suspensions after centrifugation (Fig. 7) to avoid bias due to the anisotropic arrangement of BHK-cell membranes when growing in a monolayer (Fig. 2). This estimate was obtained at a final magnification of × 22,000.

Correction of Bias Due to Section Compression: We did not correct for the effects of section compression, as no suitable circular profiles were available in BHK-cells. Section compression would not be expected to affect volume density estimates, but it might in theory lead to over-estimation of the surface density estimated by as much as 20% (2).

In a recent study, however, we have found that compression is unlikely to be significant in our sections (Griffiths, G., A. McDowall, R. Back, and J. Dubochet, manuscript in preparation). Chinese hamster ovary (CHO) cells grown in suspension are spherical. These were embedded in the same Epon mixture as used in this study. By reference to knife-marks, the direction of cutting could be ascertained. Careful measurements from micrographs indicated that there was no significant net compression occurring to the circular cell profile.

Correction of Resolution Effects: The estimation of stereological parameters on ultrathin sections is affected by the magnification at which the analysis is carried out (18). In general, more structural elements can be detected at higher magnifications up to a "critical magnification" at and beyond that by which stable structural estimates are obtained. In BHK-cells the cytoplasmic organelles can be identified much more easily and at lower magnifications than in liver cells because BHK-cells have a less dense cytoplasmic composition (Figs. 2 and 3). To find out whether we could detect ER reliably at × 22,000, we measured the volume density of ER on sections in which the ER was specifically stained with glucose-6-phosphatase (Figs. 8 and 9) (see reference

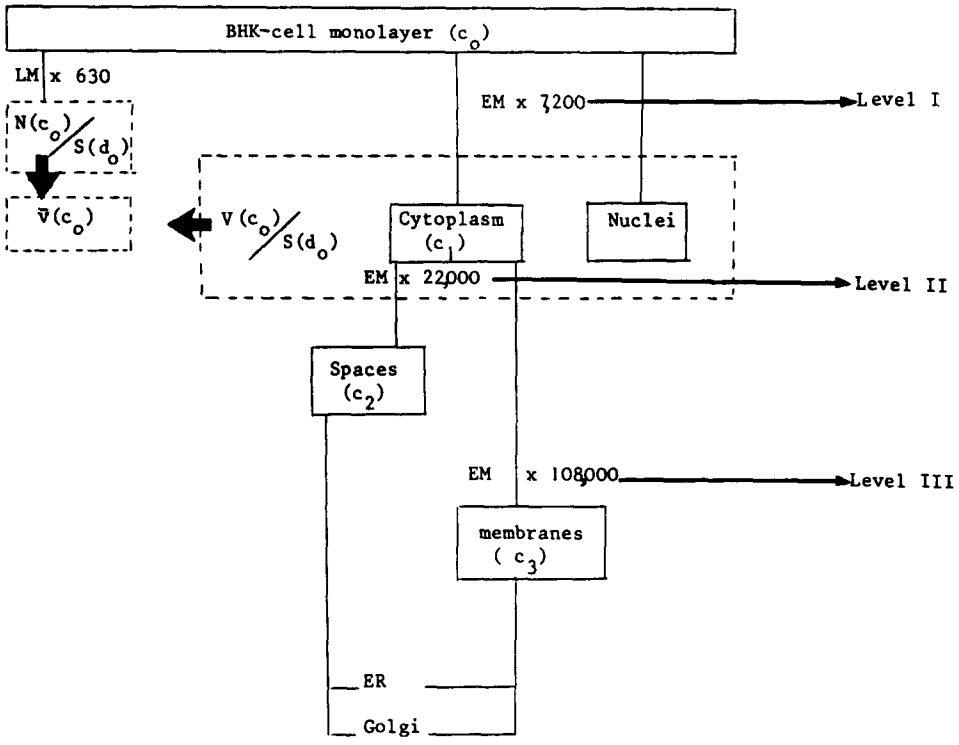

FIGURE 1 Schematic representation of the sampling method that was used (for details, see text, Materials and Methods). $N(c_0)/S(d_0)$, number of cells per unit area of dish surface; $\bar{v}(c_0)$, mean cell volume; $V(c_0)/S(d_0)$, cell volume per surface petri dish; LM, light microscopy; EM, electron microscopy.

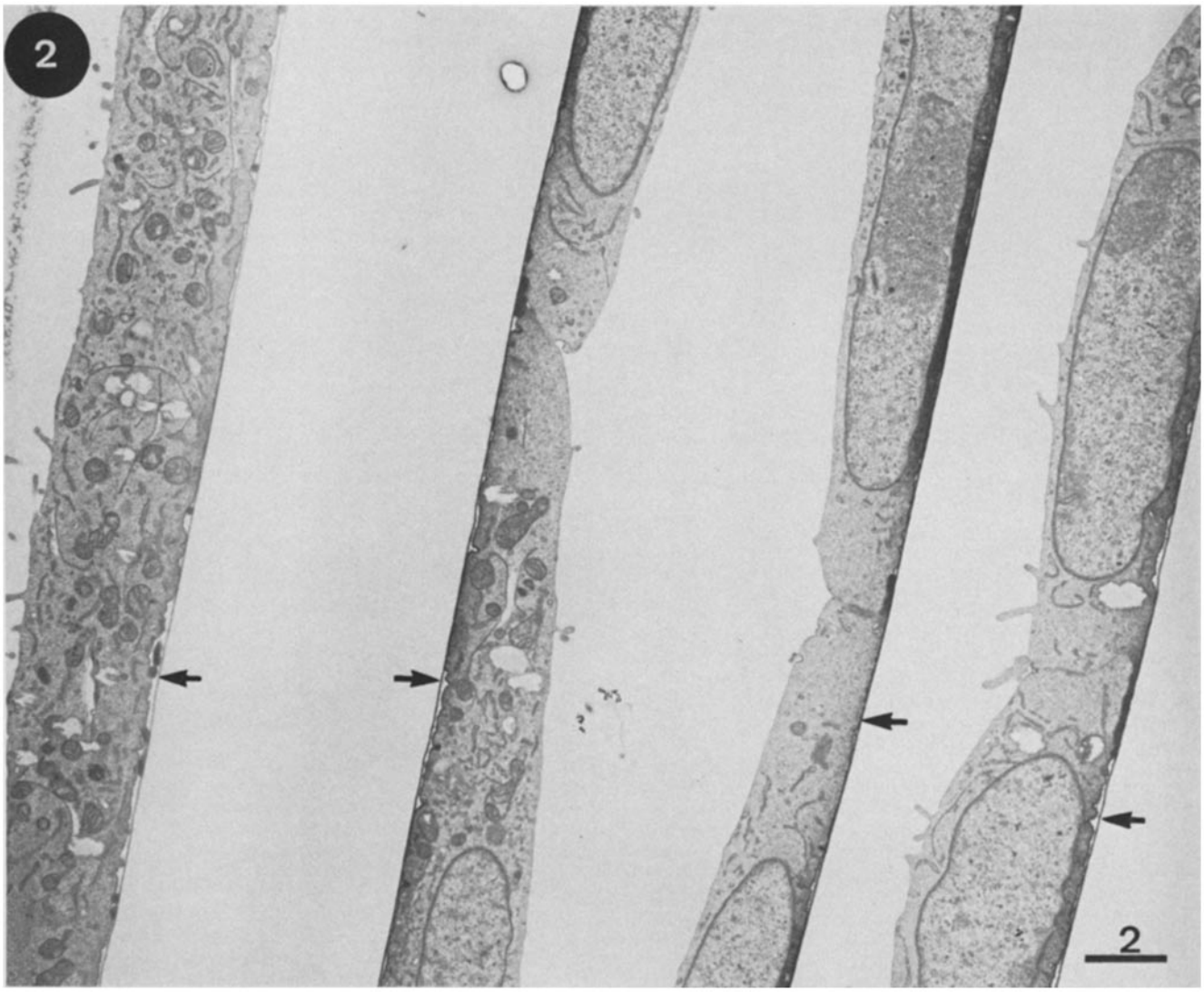

FIGURE 2 BHK cells fixed in situ. Four strips of cells are shown with the adjoining plastic from the culture plate (arrows). Bar, 2 μm. × 6,000.

10). We obtained parameter estimates for the volume density of ER (as well as surface density at × 108,000 magnification) from cytochemically treated sections that were not significantly different from those of untreated sections (results not shown). The volume density of the Golgi apparatus was also measured at × 22,000. The "Golgi stacks" can easily be identified at relatively low magnification because of their characteristic membrane pattern. They are similar in that respect to mitochondria for which it has been shown that the estimate of the surface density of their outer membranes and hence also their volume is not significantly affected by the magnification (18). The magnification of 108,000 in stage III used for the estimation of surface density both of ER and Golgi membranes was judged sufficiently high to allow for stable estimates of these variables. In liver cells where the conditions to properly allocate these membranes are more difficult, a magnification of 130,000 was required (18).

Correction of Bias Due to Section Thickness: As the stereological formulas are strictly valid only for infinitely thin sections one has to use corrections when using tissue sections with a finite section thickness ("Holmes effect," 12). Corrections for section thickness may be quite considerable when the structures to be analyzed are of the same order of magnitude or smaller than the section thickness (for a review see reference 24, chapter 4). We calculated the correction factors for section thickness both for volume and surface densities of ER and Golgi stacks. The measurements of the characteristic dimensions required for these calculations were done on 40 selected profiles of both ER and Golgi at a final magnification of 108,000 according to Weibel and Paumgartner (27). We assumed both structures to be "discrete", not "interpenetrating" and applied formulae 4.71 and 4.72, respectively, according to Weibel (25, chapter 4). The estimates of the characteristic dimensions as well as the correction factors are contained in Table I.

FIGURES 3–6 Figs. 3–5 are micrographs of one mock-infected BHK cell in situ. The small arrow in Fig. 4 indicates the plastic from the dish. The larger arrows in Figs. 3–5 point to the same Golgi stack, which is magnified in Fig. 5. Arrowheads in Figs. 4 and 5 point to the rough endoplasmic reticulum whose luminal content appears more electron dense than Golgi content and can usually be easily distinguished, even at low magnification. The tannic acid treatment makes membranes distinct but ribosomes less distinct. Fig. 6 shows part of the rough ER from a cell adjacent to that in Figs. 3–5 and at the same magnification as Fig. 5 (level 3). The small arrows indicate ribosomes whose structure is characteristically very poorly constrasted (or destroyed) by the tannic acid treatment. × 6,000 (Fig. 3); × 17,600 (Fig. 4); × 103,000 (Figs. 5 and 6).

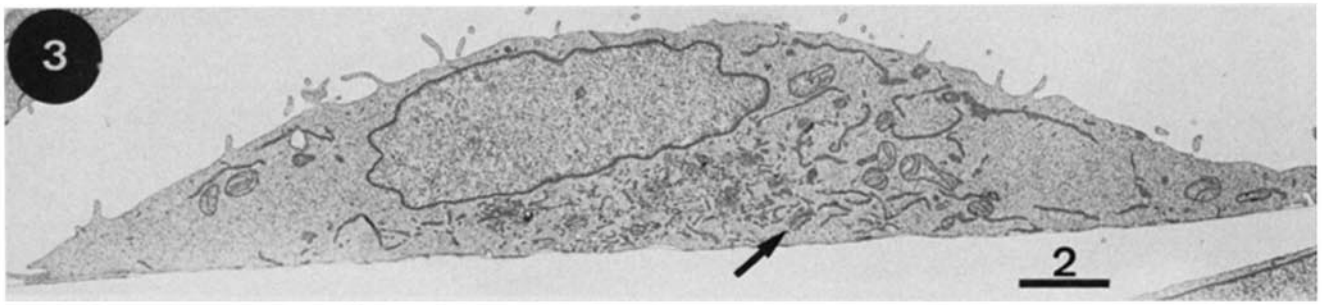
3
2

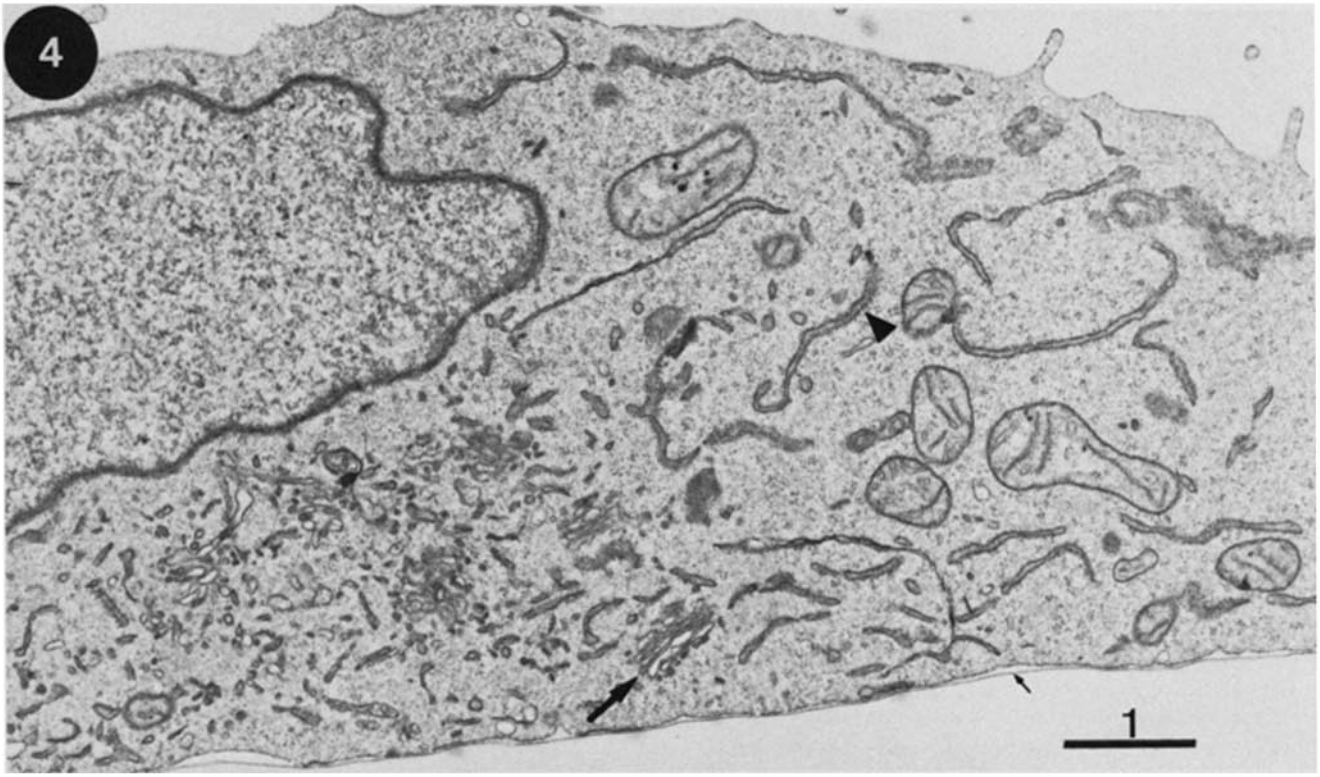
4
1

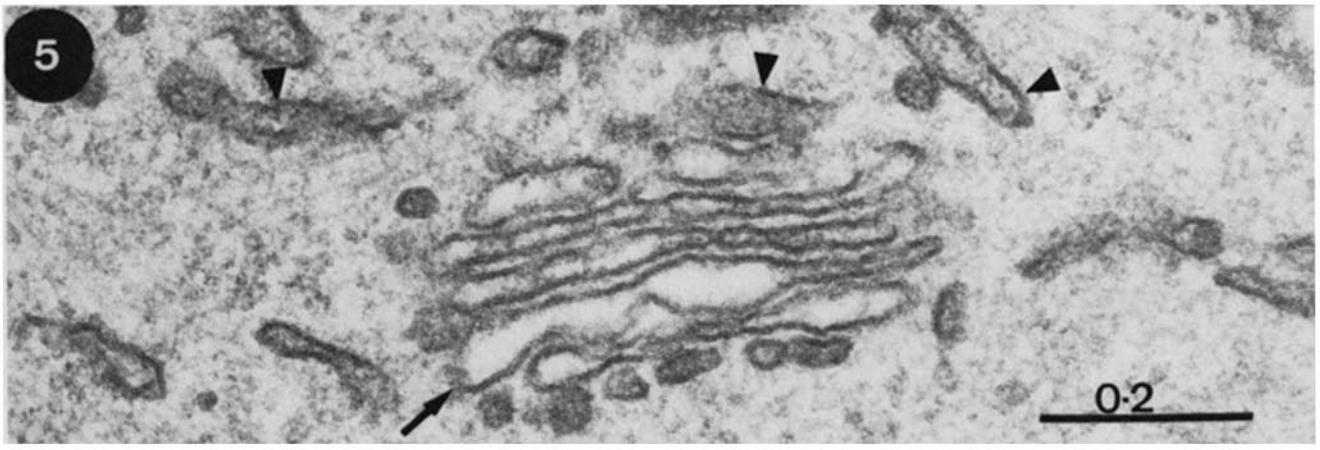
5
0·2

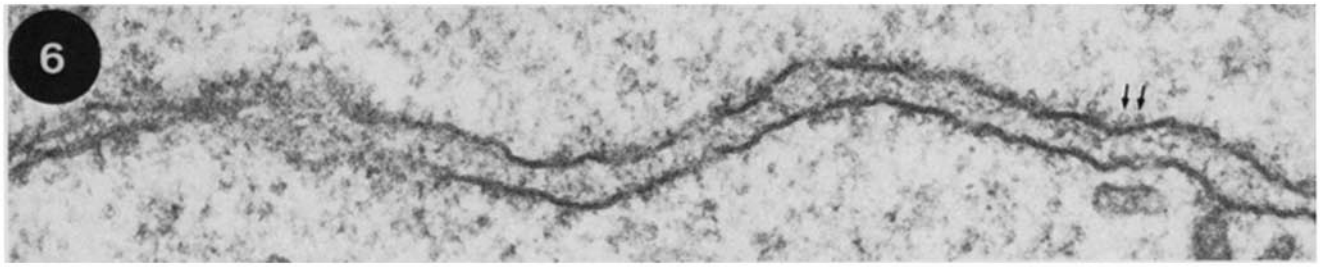
6

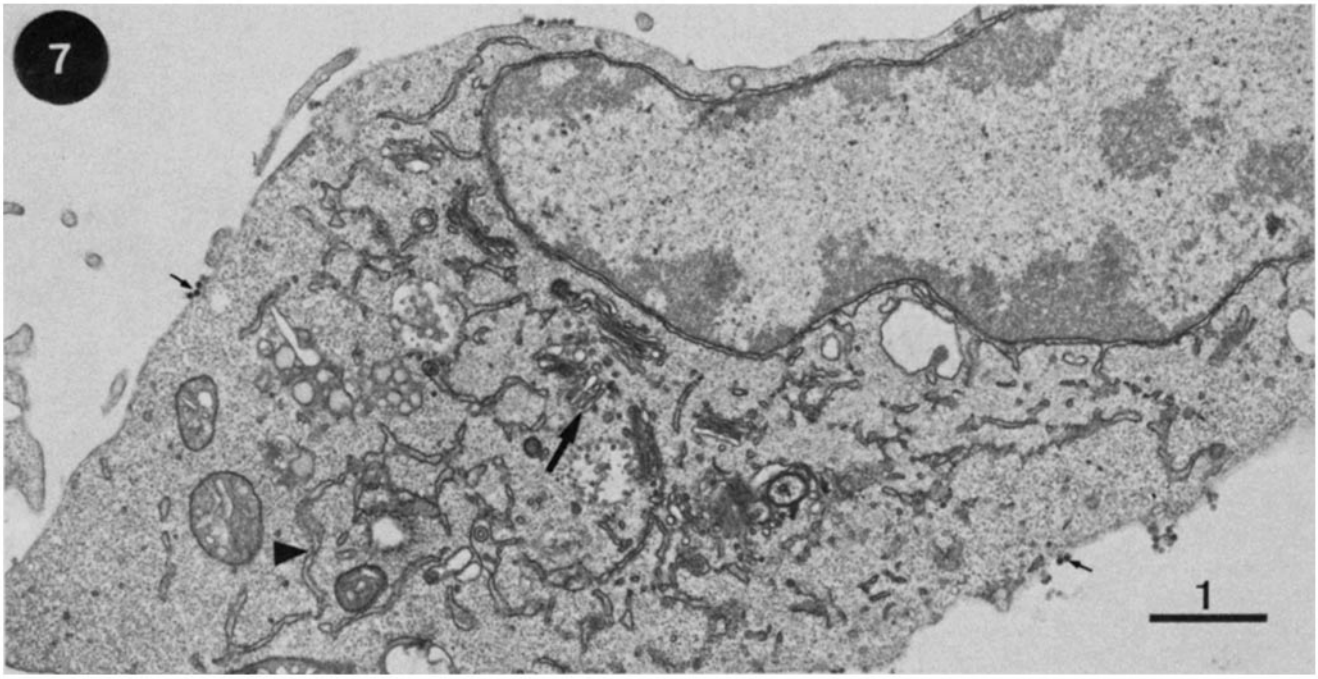

FIGURE 7 BHK cell infected with SFV and fixed as a pellet after proteinase K treatment. Small arrows indicate budded virions on the surface of the cell. The large arrow indicates a Golgi stack. Arrowhead points to cisternae of the rough ER. × 15,500.

SUMMARY OF RESULTS

A summary of the estimates obtained is given in Table II. These relative values are converted to absolute values in Table III after correcting for section thickness. With respect to the in situ cells, there was no significant difference between mock-infected and infected cells with the exception of the number of cells which is slightly reduced after infection (Table II).

The infected cells in the pellet, which were only necessary here for estimating the plasma membrane surface area showed significantly higher rates for both volume of cytoplasm per volume cell as well as surface of Golgi per volume of golgi and a significantly lower value for the volume of Golgi per volume cell (Table II). Presumably these differences reflect changes caused by the proteinase treatment and/or centrifugation process prior to fixation.

DISCUSSION

We have estimated the surface area of the membranes of endoplasmic reticulum, the Golgi complex, and the plasma membrane. Our stereological rationale was to calculate the mean cell volume for the in situ cells by taking advantage of the fact that their plastic support film is visible in the Epon sections. This fact was critical in enabling us to obtain our estimates of organelle surface areas in absolute units. This approach has the advantage that unlike many other techniques for estimating cell volume (e.g., reference 3), it makes no assumptions about the overall shape of the cells. In principle, the technique could be used for any tissue culture cell that grows on a flat plastic substrate and hence may have general applicability in stereological studies of tissue culture cells.

Having estimated mean cell volume it was then a straightforward stereological problem to estimate the volume- and surface densities of ER and Golgi. For the plasma membrane, however, because of the potential error due to isotropic sectioning of the monolayer, we chose a different strategy. This involved removing the monolayer with proteinase K on ice and then sedimenting the cells prior to fixation. By sectioning this pellet, which was assumed to be completely anisotropic, the surface to volume ratio of the cells could be easily estimated. Since we had no independent method for estimating mean cell volume of these cells, we had to assume that this parameter did not change during the proteinase treatment and centrifugation procedure. This may not be a valid assumption and any difference in absolute cell volume caused by this procedure (e.g., uptake, or loss of water) could effect a corresponding error in all the absolute volume and surface estimates for these cells, including of course the surface area of the plasma membrane. Indeed, the significant differences between the volume of cytoplasm per volume of these cells from the pellet with the in situ cells may reflect a real difference in mean cell volume. We are presently trying to develop an alternative technique for independently estimating the mean cell volume of BHK-cells after centrifugation to overcome this problem.

Fortunately, the above reservations do not apply to the two organelles which are most interesting for the subsequent biochemical analysis, the ER, and Golgi complex. For both these organelles, the potential errors rest with the problem of identification. The ER is often contiguous with the Golgi stacks and the only clear difference between the two organelles is a slight contrast difference with our contrasting procedure (see Fig. 5). That the estimate of ER volume- and surface-densities from cells treated cytochemically for glucose-6-phosphatase, an ER-marker, was the same as untreated cells was therefore reassuring. For the Golgi complex our measurements relate to Golgi stacks plus vesicular profiles in close proximity to the stack. Precisely where the Golgi zone begins and ends is admittedly subjective: future analysis should concentrate on using specific markers for different compartments of the Golgi complex.

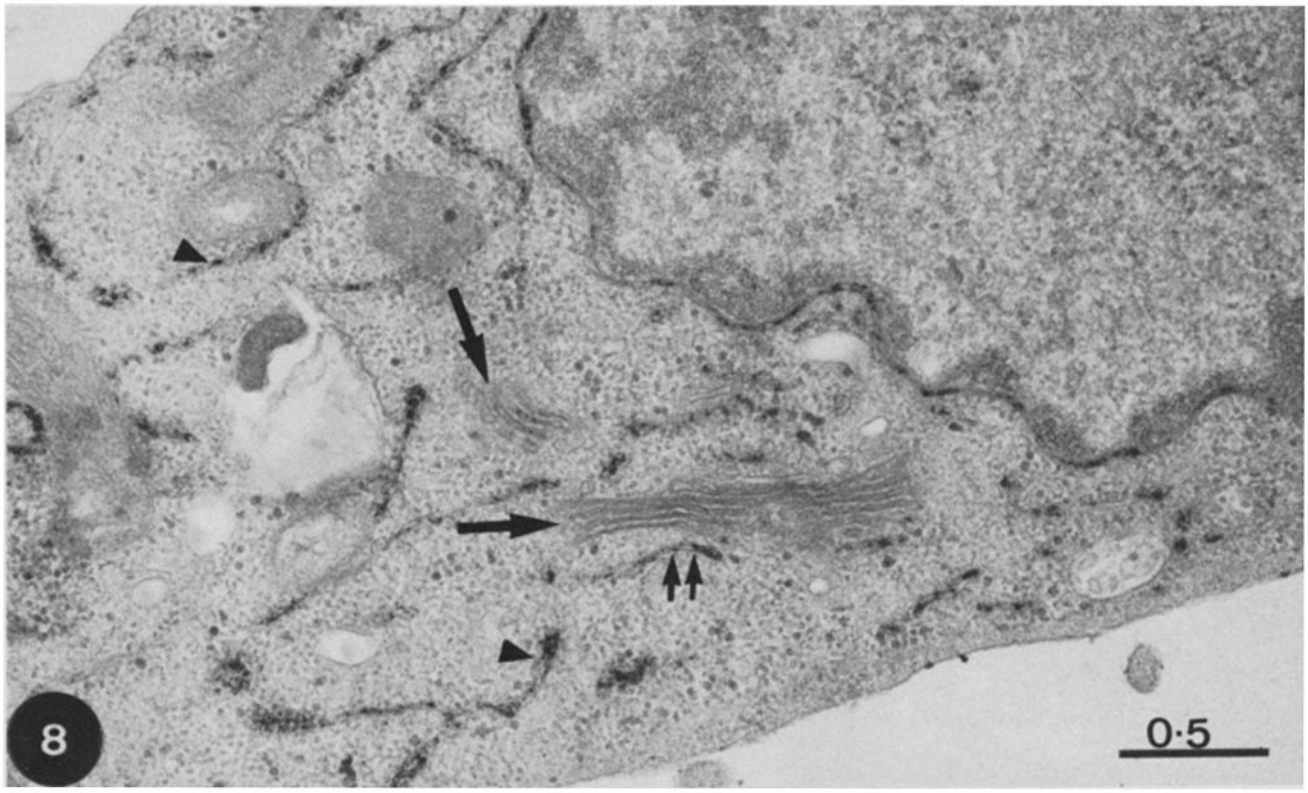

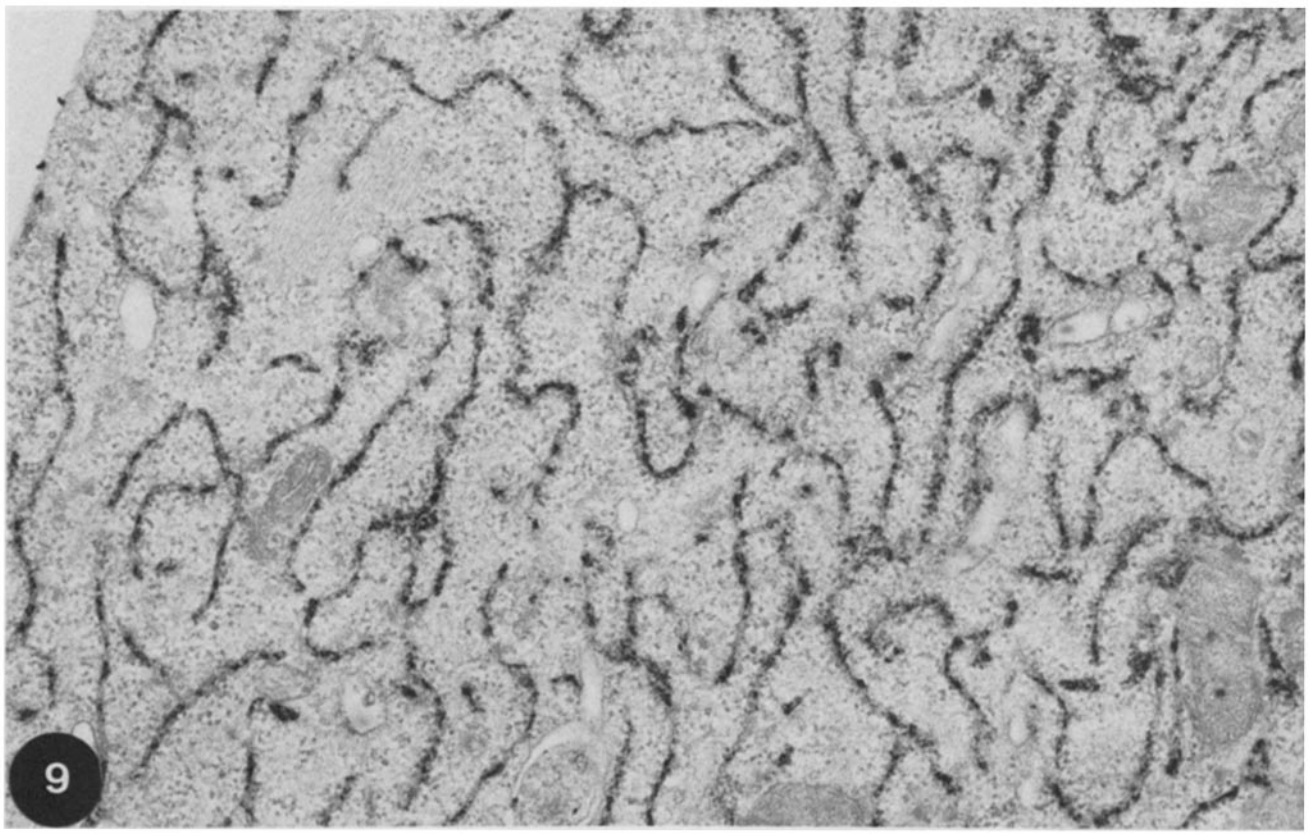

FIGURES 8 and 9 Mock-infected BHK cells treated cytochemically for glucose-6-Pase. In Fig. 8, which is from the perinuclear region, the ER (arrowhead) and nuclear envelope is fairly uniformly contrasted with the lead reaction product but the Golgi stacks (large arrows) have characteristically only spotty reaction product. The reactive cisternae, which are usually found in close vicinity of the Golgi stacks (double arrows), are here interpreted (and measured) as ER. In Fig. 9, a part of the cell away from the cell body, which has always more ER (arrowhead) than the perinuclear region, is shown after the cytochemical reaction. × 40,000.

TABLE I

Derivation of Correction Factors for Section Thickness Effect

	ER cisternae	Golgi cisternae	Golgi stack
Model structure	disk	disk	disk
$\bar{d}$, nm (± SD)	34 ± 6.4	26 ± 4.3	199 ± 44
D, nm	1,500	800	800
$= D/\bar{d}$	44	31	4
Section thickness			
t, nm (± SD)	40.5 ± 2.3	40.5 ± 2.3	40.5 ± 2.3
$g = t/\bar{d}$	1.19	1.56	0.20
Correction factors			
$K_t (V_V)$	0.62	—	0.87
$K_t (S_V)$	0.95	0.91	—

For explanation of symbols see Weibel (24).

There were no significant differences between the values obtained for mock-infected and SFV-infected cells, showing that 6 h infection does not alter the size of these major compartments. These estimates for membrane surface areas of the major compartments known to be involved in intracellular transport now provide a basis for estimating spike protein densities, which is dealt with in the accompanying paper (20).

APPENDIX

Complete stereological formulas used to calculate the relevant parameters at the sampling levels I–III:

LEVEL I

$$\frac{V(c_1)}{V(c_0)} = \frac{\frac{a_1}{p_1} \cdot \sum_{i=i}^{m} P_i(c_1) \cdot M_i^{-2}}{\frac{a_1}{p_1} \cdot \sum_{i=1}^{m} P_i(c_0) \cdot M_i^{-2}} \tag{7}$$

LEVEL II*a*

$$\frac{V(c_2)}{V(c_1)} = \frac{\frac{a_2}{p_2} \cdot \sum_{i=1}^{m} P_i(c_2) \cdot M_i^{-2}}{\frac{a_1}{p_1} \cdot \sum_{i=1}^{m} P_i(c_1) \cdot M_i^{-2}} \tag{8}$$

LEVEL II*b*

$$\frac{S(\partial c_0)}{V(c_0)} = \frac{2 \cdot \frac{a_1}{l_1} \cdot \sum_{i=1}^{m} I_i(\partial c_0) \cdot M_i^{-1}}{\frac{a_1}{p_1} \cdot \sum_{i=1}^{m} P_i(c_0) \cdot M_i^{-2}}, \tag{9}$$

LEVEL III

$$\frac{S(\partial c_3)}{V(c_2)} = \frac{2 \cdot \frac{a_3}{l_3} \cdot \sum_{i=1}^{m} I_i(\partial c_3) \cdot M_i^{-1}}{\frac{a_3}{p_3} \cdot \sum_{i=1}^{m} P_i(c_2) \cdot M_i^{-2}} \tag{10}$$

where

P_i and I_i are the number of points and intersections, respectively counted in the i^{th} quadrat. M_i is the precise magnification of micrograph of the i^{th} quadrat. (Precise values for each level are given in the text.) m is the number of micrographs (24; in all levels) and a, l, and p are constants characterizing test systems (5, 24). Subscript 1 to constants a, l, and p indicates test system D64, coarse lattice, total number of test points per micrograph is 64; subscript 2 to constants a, l, p indicates test system D64, fine lattice for points on ER and Golgi; total number of test points 1024; Subscript 3 to constants a, l, p indicates test system C64, the fine lattice of lines was used; total number of test points 576; S and V, surface and volume, respectively.

TABLE II

Estimation of Relative Values

Treatment	$N(c_0)/S(d_0)$	$V(c_0)/S(d_0)$	$V_v(cy,c)$	$V_v(er,c)$	$V_v(go,c)$	$S_v(er,c)$	$S_v(go,c)$	$S_v(pm,c)$
Units	cm^{-2}	*cm*				mm^{-1}	mm^{-1}	mm^{-1}
BHK-control mock-infected monolayer	2.6×10^5 ± 2.1×10^4	1.014×10^{-2} ± 4.5×10^{-4}	0.7280* ± 0.029	0.1400 ± 0.0158	0.0350 ± 0.009	53,600‡ ± 1,260	27,300§ ± 1,260	
BHK-SFV monolayer	2.3×10^5§ ± 1.8×10^4	8.76×10^{-3} ± 5×10^{-4}	0.7240 ± 0.028	0.1330 ± 0.00125	0.0290 ± 0.005	55,600 ± 4,000	28,400 ± 1,000	
BHK-SFV pellet			0.7740§ ± 0.014	0.1450 ± 0.0104	0.0190§ ± 0.004	54,800 ± 5,750	33,500 ± 1,560	890 ± 35

$N(c_0)/S(d_0)$, number of cells per unit area of dish surface; $V(c_0)/S(d_0)$, volume of cells per unit area of dish surface; $V_v(cy,c)$, $V_v(er,c)$, $V_v(go,c)$, volumes of cytoplasm, ER, and Golgi, respectively, per unit cell volume; $S_v(er,c)$, $S_v(go,c)$, $S_v(pm,c)$, surface of ER, Golgi, and plasma membrane, respectively per unit cell volume. Note that these are conventional letter notations (25) for the more general notation used in the method and appendix.

* These volume ratios can be converted to percent. Hence, V_{cy}/V_{cell} 0.7 means that 70% of the volume of the cell consists of cytoplasm; conversely 30% is made up of nucleus.

‡ Values indicate surface for every cubic millimeter of volume of the organelle.

§ Significantly different at 5, and 0.1% level, respectively, from other values in the same column by student's t test.

TABLE III

Average Cell Estimates

Treatment	Volume cell	Volume ER	Volume Golgi	Surface area of ER	Surface area of Golgi	Surface area of plasma membrane
	μm^3	μm^3	μm^3	μm^2	μm^2	μm^2
BHK mock-infected monolayer	3,900 ± 360	246 ± 29	85 ± 23	20,200 ± 2,600	2,440 ± 640	
BHK-SFV monolayer	3,809 ± 400	227 ± 25	69 ± 17	19,400 ± 2,200	2,050 ± 500	
BHK-SFV free cells (pellet)	3,809 ± 400*	264 ± 19	48 ± 11‡	22,170 ± 2,000	1,670 ± 450‡	3,400 ± 350

* This is assumed to be the same as for the monolayer.

‡ Significantly different at 5, and 0.1% level, respectively, from other values in the same column by students t test (23 degrees of freedom).

This project was started following a kind invitation from Dr. Ewald Weibel. We thank him warmly for his interest and many helpful suggestions. We must also thank Dr. Luis Cruz-Orive whose expertise proved invaluable in providing the theoretical background to the stereology. A number of useful changes were introduced after Drs. Jacques Dubochet, Kevin Leonard, Terry Mayhew, and Steve Fuller critically read the manuscript. The method of removing the monolayer cells using propylene oxide was described to us by Dr. Joe Sanger. Finally, thanks are due to Annemette Ohlsen and Ruth Giovanelli for technical assistance.

Received for publication 7 November 1983, and in revised form 7 March 1984.

REFERENCES

1. Bolender, R. P. 1974. Stereological analysis of the guinea pig pancreas. I. Analytical model and quantitative description of nonstimulated pancreatic exocrine cells. *J. Cell Biol.* 61:269–287.
2. Bolender, R. P., D. Paumgartner, G. Losa, D. Muellener, and E. R. Weibel. 1978. Integrated stereological and biochemical studies on hepatocytic membranes. I. Membrane recoveries in subcellular fractions. *J. Cell Biol.* 77:565–589.
3. Buschmann, R. J., and D. J. Mancke. 1981. Morphometric analysis of the membranes and organelles of small intestine enterocytes. II. Lipid fed hamsters. *J. Ultrastruct. Res.* 76:15–26.
4. Cochran, W. G. 1977. Sampling Techniques. John Wiley and Sons, London.
5. Cruz-Orive, L. M. 1982. The use of quadrats and test systems in stereology, including magnification corrections. *J. Microsc.* 125:89–102.
6. Cruz-Orive, L. M., and E. R. Weibel. 1981. Sampling designs for stereology. *J. Microsc.* 122:235–272.
7. Farquhar, M. G., and G. Palade. 1981. The Golgi apparatus (complex) (1954–1981) from artefact to center stage. *J. Cell Biol.* 91:77s–103s.
8. Green, J., G. Griffiths, D. Louvard, P. Quinn, and G. Warren. 1981. Passage of viral membrane proteins through the Golgi complex. *J. Mol. Biol.* 152:663–698.
9. Griffiths, G., R. Brands, B. Burke, D. Louvard, and G. Warren. 1982. Viral membrane proteins acquire galactose in *trans* Golgi cisternae during intracellular transport. *J. Cell Biol.* 95:781–792.
10. Griffiths, G., P. Quinn, and G. Warren. 1983. Dissection of the Golgi complex. I. Monensin inhibits the transport of viral membrane proteins from *medial* to *trans* Golgi cisternae in Baby hamster kidney cells infected with Semliki Forest virus. *J. Cell Biol.* 96:835–850.
11. Gunderson, H. J. G. 1977. Notes on the estimation of the numerical density of arbitrary profiles: the edge effect. *J. Microsc.* 111:219–223.
12. Holmes, A. 1927. Petrographic Methods and Calculations. Murphy, London.
13. Kreibich, G., P. Debey, and D. Sabatini. 1973. Selective release of content from microsomal vesicles without membrane disassembly. I. Permeability changes induced by low detergent concentrations. *J. Cell Biol.* 58:436–462.
14. Meldolesi, J., N. Borgese, P. De Camilli, and B. Ceccarelli. 1978. Cell surface reviews 5. Membrane Fusion Poste, G., and G. L. Nicolson, editors. 509–627.
15. Meldolesi, J., J. D. Jamieson, and G. E. Palade. 1971. Composition of cellular membranes in the pancreas of the guinea pig. I. Isolation of membrane fractions. *J. Cell Biol.* 49:109–129.
16. Müller, A. E., L. M. Cruz-Orive, P. Gehr, and E. R. Weibel. 1981. Comparison of two sub-sampling methods for electron microscopic morphometry. *J. Microsc.* 123:35–42.
17. Palade, G. E. 1975. Intracellular aspects of the process of protein synthesis. *Science (Wash. DC)* 189:347–357.
18. Paumgartner, D., G. Losa, and E. R. Weibel. 1981. Resolution effects on the stereological estimation of surface and volume and its interpretation in terms of fractal dimensions. *J. Microsc.* 121:51–59.
19. Quinn, P., G. Griffiths, and G. Warren. 1983. Dissection of the Golgi complex. II. Density separation of specific Golgi functions in virally infected cells treated with monensin. *J. Cell Biol.* 96:851–856.
20. Quinn, P., G. Griffiths, and G. Warren. 1984. Density of newly synthesized membrane proteins in intracellular membranes. *J. Cell Biol.* 98:0000–0000.
21. Rothman, J. E. 1981. The Golgi apparatus: two organelles in tandem. *Science (Wash DC).* 213:1212–1219.
22. Simoniescu, N., and M. Simionescu. 1976. Galloylglucases of low molecular weight as mordants in electron microscopy. *J. Cell Biol.* 70:608–621.
23. Small, J. V. 1968. Measurement of section thickness. *In* Proceedings of the 4th European Congress on Electron Microscopy. D. S. Bocciarelli, editor. Tipografia Poliglotta Vaticana, Roma. 609–615.
24. Smith, C. S., and L. Guttman. 1953. Measurement of ineternal boundaries in three dimensional structures by random sectioning. *Trans. Am. Inst. Mech. Eng.* 197:81–88.
25. Weibel, E. R. 1979. Stereological Methods. I. Practical methods for biological morphometry. Academic Press, Inc. New York.
26. Weibel, E. R., W. Staubli, H. R. Gnagi, and F. A. Hess. 1969. Correlated morphometric and biochemical studies on the liver cell. I. Morphometric model, stereologic methods and normal morphometric data for rat liver. *J. Cell Biol.* 42:68–91.
27. Weibel, E. R., and D. Paumgartner. 1978. Integrated stereological and biochemical studies on hepatocyte membranes. II Correction of section thickness effect on volume and surface density estimates. *J. Cell Biol.* 77:584–597.